Supplementary Information

Spatial coupling between DNA replication and mismatch repair in *Caulobacter crescentus*

Tiancong Chai, Céline Terrettaz and Justine Collier

Content:

Supplementary Tables (page 2)

Table S1 (page 2)

Table S2 (page 3)

Table S3 (page 4)

Table S4 (page 5)

Supplementary Figures with legends (page 6)

Fig.S1 (page 6)

Fig.S2 (page 8)

Fig.S3 (page 9)

Fig.S4 (page 10)

Fig.S5 (page 11)

Fig.S6 (page 12)

Fig.S7 (page 13)

Fig.S8 (page 14)

Supplementary Materials and Methods (page 15)

Supplementary References (page 16)

Supplementary Tables

Table S1: Oligonucleotides used in this study. Restriction enzyme recognition sites used for cloning purposes are underlined.

Name	Sequence (5'→3')	Use
CT1	GGTAAGCTTGGTCCGCGTGGGGATCTCTAC (HindIII)	Construction of pNPTS138-ΔmutS
CT2	CCCGGATCCGGGCGGCGTTAAGGAATTACAC (BamHI)	
CT3	CCCGGATCCTAGCGGGTACCCATATAGA (BamHI)	
CT4	CGGGCTAGCAACCCAGATCCCACAACGCATAC (NheI)	
CT8	CGGGCTAGCCGAGACGATGGATGACAAACACC (NheI)	Construction of pNPTS138-ΔmutL
CT10	GGTAAGCTTATGCCCATCCGCCGCCTGCCG (HindIII)	
CT11	CCCGGATCCCATGGCCTGGCGCTTGATCTCC (BamHI)	
CT12	CCCGGATCCTGAGGCCAGAGCGCCCCCTAC (BamHI)	
TC46	GTCGGATCCGCCTGATCGACAGGGCGAACCA (BamHI)	Construction of pNPTS138-ΔuvrD
TC47	CGGGAATTCCGCCGAAAAGCGAGCGTTCAGC (EcoRI)	
TC63	ATAAAGCTTATGTTTCCCGACACCGACTCGC (HindIII)	
TC64	CGTGGATCCGCGGTTCTTCCAGCCGTCGATG (BamHI)	
TC18	GCGAAGCTTGGTCCGCGTGGGGATCTCTA (HindIII)	Construction of pNPTS138-PmutS-YFP-MutS
TC19	GTGGGATCCCATGACGCCCGGAAACTACAG (BamHI)	
TC20	GAAGGATCCATGGTGAGCAAGGGCGAGGAG (BamHI)	
TC21	CTCGAATTCGGACAGCTCGACCGACGCCA (EcoRI)	
TC42	TGACTGACCGCGGCGGCGGCGGCGGCGTCCAGCTTGG	Construction of pNPTS138- MutS($_{849}$AAAAA$_{853}$) and pXYFPN4- MutS($_{849}$AAAAA$_{853}$)
TC43	CCAAGCTGGACGCCGCCGCCGCCGCCGCGGTCAGTCA	
TC52	AACAAGCTTGGTAAGTCGACCTTCCTGCGCC, HindIII	Construction of pNPTS138- MutS($_{849}$AAAAA$_{853}$)
TC53	GCGGAATTCGCTTGTAGGGCCGCAGGAACAG, EcoRI	
TC34	CGAAAGCTTCTTTCCCGGCGTCGTTGTGGA (HindIII)	Construction of pNPTS138-DnaQ(G13E)
TC35	TTTGGGTCAAACTCGGTGGTTTCG	
TC36	CGAAACCACCGAGTTTGACCCAAA	
TC37	GTGGGATCCGCCATGGCCCCTGTCGAATGG (BamHI)	
TC14	GGAAAGCTTCCAGCAGGCTCAGAATCCGAA (HindIII)	Construction of pNPTS138-PmutL-YFP-MutL
TC15	GCGGGATCCCATCAAGCGGACTTTCACGGG (BamHI)	
TC16	GACGGATCCATGGTGAGCAAGGGCGAGGA (BamHI)	
TC17	GGCGAATTCGGACTTCATGAATTTCAGGCG (EcoRI)	
JC155	CGGGTACCATGAACGCCCACGCCACGCCGACC (KpnI)	Construction of pXYFPN4-MutS, pXYFPN4-MutS($_{849}$AAAAA$_{853}$), pXYFPN4-MutS(F44A), pXYFPN4-MutS(K661M), pXYFPN4-MutS(E735A)
JC156	GGCTAGCCTAGGCCGTGAGCAGACCCTTAAGG (NheI)	
TC27	CAGCTCGTAGGCATCGCCCATGC	Construction of pXYFPN4-MutS(F44A)
TC28	GCATGGGCGATGCCTACGAGCTG	
TC23	GAAGGTCGACATACCGGCCATG	Construction of pXYFPN4-MutS(K661M)
TC24	CATGGCCGGTATGTCGACCTTC	
TC38	ATCCTGGACGCCATCGGCCGGG	Construction of pXYFPN4-MutS(E735A)
TC39	CCCGGCCGATGGCGTCCAGGAT	
CoC-7_1	TCGGTACCATGCCCATCCGCCGCCTGCCG (KpnI)	Construction of pXYFPN4-MutL, pXYFPN4-MutL($_{497}$ATLAAP$_{502}$), pXYFPN4-MutL(D472N) and pXYFPN4-MutL(D472N, $_{497}$ATLAAP$_{502}$)
CoC-8_4	GGAGCTCTGGCCTCACCGCCGCCCGAACAGC (SacI)	
TC40	ACCTCGGGGGCGGCCAGGGTGGCGCGGGTC	Construction of pXYFPN4- MutL($_{497}$ATLAAP$_{502}$) and pXYFPN4-MutL(D472N, $_{497}$ATLAAP$_{502}$)
TC41	GACCCGCGCCACCCTGGCCGCCCCCGAGGT	
TC31	CGCGTGCTGGTTGACAATGAC	Construction of pXYFPN4-MutL(D472N) and pXYFPN4-MutL(D472N, $_{497}$ATLAAP$_{502}$)
TC32	GGTCATTGTCAACCAGCACGCG	
TC54	TAGGTACCATGTTTCCCGACACCGACTCGC (KpnI)	Construction of pXYFPN4-UvrD
TC55	CCCGCTAGCTCAGGCCTTCTCGACGAAGCTG (NheI)	

Table S2: Plasmids used in this study.

Plasmid name	Description	Source
pNPTS138	Suicide vector carrying the *sacB* gene	D. Alley, unpublished
pNPTS138-ΔmutS	pNPTS138 derivative used to create the *ΔmutS* deletion strain	This study
pNPTS138-ΔmutL	pNPTS138 derivative used to create the *ΔmutL* deletion strain	This study
pNPTS138-ΔuvrD	pNPTS138 derivative used to create the *ΔuvrD* deletion strain	This study
pNPTS138-PmutS-YFP-MutS	pNPTS138 derivative used to replace *mutS* by *yfp-mutS* (under the control of native *mutS* promoter)	This study
pNPTS138-DnaQ(G13E)	To replace native *dnaQ (CCNA_00005)* with *dnaQ(G13E)* allele	This study
pNPTS138-MutS($_{849}$AAAAA$_{853}$)	To replace native *mutS* with the *mutS($_{849}$AAAAA$_{853}$)* allele	This study
pNPTS138-PmutL-YFP-MutL	pNPTS138 derivative used to replace *mutL* by *yfp-mutL* (under the control of native *mutL* promoter)	This study
pXYFPN4	For integrating constructs encoding N-terminal YFP fusions under the control of the native *xylX* promoter	(1)
pXYFPN4-MutS	*mutS* cloned into pXYFPN4	This study
pXYFPN4-MutS($_{849}$AAAAA$_{853}$)	*mutS($_{849}$AAAAA$_{853}$)* cloned into pXYFPN4	This study
pXYFPN4-MutS(F44A)	*mutS(F44A)* cloned into pXYFPN4	This study
pXYFPN4-MutS(K661M)	*mutS(K661M)* cloned into pXYFPN4	This study
pXYFPN4-MutS(E735A)	*mutS(E735A)* cloned into pXYFPN4	This study
pXYFPN4-MutL	*mutL* cloned into pXYFPN4	This study
pXYFPN4-MutL($_{497}$ATLAAP$_{502}$)	*mutL($_{497}$ATLAAP$_{502}$)* cloned into pXYFPN4	This study
pXYFPN4-MutL(D472N)	*mutL(D472N)* cloned into pXYFPN4	This study
pXYFPN4-MutL(D472N, $_{497}$ATLAAP$_{502}$)	*mutL(D472N, $_{497}$ATLAAP$_{502}$)* cloned into pXYFPN4	This study
pXYFPN4-UvrD	*uvrD* cloned into pXYFPN4	This study

Table S3: Strains used in this study.

Strain name	Genotype	Source
Escherichia coli		
TOP10	*F- mcrA Δ(mrr-hsdRMS-mcrBC) φ80lacZΔM15 ΔlacX74 nupG recA1 araD139 Δ(ara-leu)7697 galE15 galK16 rpsL(Str^R) endA1 λ$^-$*	Invitrogen (USA)
Caulobacter crescentus		
NA1000	Synchronizable derivative of wild-type strain CB15 (CB15N)	(2)
JC1427	NA1000 *ΔmutS*	This study
JC1426	NA1000 *ΔmutL*	This study
JC1575	NA1000 *ΔmutS ΔmutL*	This study
JC1847	NA1000 *ΔuvrD*	This study
JC1986	NA1000 *ΔuvrD ΔmutL*	This study
JC1784	NA1000 *YFP-mutS*	This study
JC1433	NA1000 Δ*mutS Pxyl::YFP-mutS*	This study
JC577	NA1000 *dnaN-CFP*	(3)
JC1625	NA1000 *dnaN-CFP* Δ*mutS Pxyl::YFP-mutS*	This study
JC1770	NA1000 Δ*mutS Pxyl::YFP-mutS*($_{849}$*AAAAA*$_{503}$)	This study
JC1799	NA1000 *mutS*($_{849}$*AAAAA*$_{503}$)	This study
JC1678	NA1000 *dnaQ(G13E)*	This study
JC1724	NA1000 Δ*mutS Pxyl::YFP-mutS* pNPTS138-DnaQ(G13E) integrated at *dnaQ* locus	This study
JC1666	NA1000 Δ*mutS Pxyl::YFP-mutS(F44A)*	This study
JC1669	NA1000 *dnaN-CFP* Δ*mutS Pxyl::YFP-mutS(F44A)*	This study
JC1665	NA1000 Δ*mutS Pxyl::YFP-mutS(K661M)*	This study
JC1739	NA1000 Δ*mutS Pxyl::YFP-mutS(E735A)*	This study
JC1668	NA1000 *dnaN-CFP* Δ*mutS Pxyl::YFP-mutS(K661M)*	This study
JC1740	NA1000 *dnaN-CFP* Δ*mutS Pxyl::YFP-mutS(E735A)*	This study
JC1769	NA1000 *YFP-mutL*	This study
JC1825	NA1000 Δ*mutL Pxyl::YFP-mutL*	This study
JC1812	NA1000 *dnaN-CFP* Δ*mutL Pxyl::YFP-mutL*	This study
JC1805	NA1000 *dnaN-CFP* Δ*mutS* Δ*mutL Pxyl::YFP-mutL*	This study
JC1749	NA1000 Δ*mutL Pxyl::YFP-mutL*($_{497}$*ATLAAP*$_{502}$)	This study
JC1750	NA1000 *dnaN-CFP* Δ*mutL Pxyl::YFP-mutL*($_{497}$*ATLAAP*$_{502}$)	This study
JC1667	NA1000 Δ*mutL Pxy::YFP-mutL(D472N)*	This study
JC1670	NA1000 *dnaN-CFP* Δ*mutL Pxy::YFP-mutL(D472N)*	This study
JC1894	NA1000 *dnaN-CFP* Δ*mutS* Δ*mutL Pxy::YFP-mutL(D472N)*	This study
JC1753	NA1000 *dnaN-CFP* Δ*mutL Pxyl::YFP-mutL(D472N,* $_{497}$*ATLAAP*$_{502}$)	This study
JC1870	NA1000 Δ*uvrD Pxyl::YFP-uvrD*	This study
JC1846	NA1000 *Pxyl::YFP-uvrD*	This study
JC2211	NA1000 *Pxyl::YFP-uvrD* pNPTS138-DnaQ(G13E) integrated at *dnaQ* locus	This study
JC1977	NA1000 Δ*mutS Pxyl::YFP-uvrD*	This study

Table S4: Comparison of spontaneous mutation rates of *C. crescentus* strains used in this study. The symbols * and # indicate that the mutation rate is statistically significantly different or equivalent, respectively, to that of the NA1000 (WT) reference strain (for Zones A and D), of the JC1433 (*ΔmutS Pxyl::YFP-mutS)* strain (Zone B) or of the JC1825 *(ΔmutL Pxyl::YFP-mutL)* strain (Zone C). Student's *t*-tests were used to estimate statistical significance: differences were considered as significant (*) if P<0.05. The "relative mutation rate" value, facilitating comparisons, was calculated setting the spontaneous mutation rate of the NA1000 (WT) strain to a value of 1 (arbitrary units).

Zone	Strain number	Genotype (disturbed activity)	Number of Rif^R colonies * 10^{-9} total colonies [±standard deviation]	Relative mutation rate [% of DNA repair activity]
A	NA1000	WT	8.3 [±2.8]	1 [=100%]
	JC1427	*ΔmutS*	998.3 [±212.9]*	120.3 [=0%]
	JC1426	*ΔmutL*	916.7 [±312.4]*	110.4 [=0%]
	JC1575	*ΔmutS ΔmutL*	1152.7 [±423.1]*	138.9
	JC1847	*ΔuvrD*	540.1 [±95.0]*	65.1 [=0%]
	JC1986	*ΔuvrD ΔmutL*	1979.3 [±460.0]*	238.5
	JC577	*dnaN-CFP*	55.8 [±33.6]#	6.7
	JC1784	*YFP-mutS*	52.8 [±21.4]#	6.4 [95.5%]
	JC1799	*mutS($_{849}$AAAAA$_{853}$)* (β-clamp binding)	56.8 [±24.3]*	6.8 [95.1%]
	JC1678	*dnaQ(G13E)*	3973.3 [±1466.0]*	478.7
	JC1769	*YFP-mutL*	148.6 [±78.1]#	17.9 [84.6%]
	JC2212	*mutL($_{497}$ATLAAP$_{502}$)* (β-clamp binding)	932.7 [±315.6]*	112.4 [~0%]
B	JC1433	*ΔmutS Pxyl::YFP-mutS*	24.2 [±9.9]	2.9 [98.4%]
	JC1770	*ΔmutS Pxyl::YFP-mutS($_{849}$AAAAA$_{853}$)* (β-clamp binding)	45.0 [±21.2]#	5.4 [96.3%]
	JC1666	*ΔmutS Pxyl::YFP-mutS(F44A)* (mismatch recognition)	843.0 [±313.2]*	101.6 [15.7%]
	JC1665	*ΔmutS Pxyl::YFP-mutS(K661M)* (nucleotide binding and ATP hydrolysis)	792.3 [±75.0]*	95.5 [20.8%]
	JC1739	*ΔmutS Pxyl::YFP-mutS(E735A)* (ATP hydrolysis)	917.0 [±340.0]*	110.5 [8.2%]
C	JC1825	*ΔmutL Pxyl::YFP-mutL*	56.3 [±28.5]	6.8 [94.7%]
	JC1749	*ΔmutL Pxyl::YFP-mutL($_{497}$ATLAAP$_{502}$)* (β-clamp binding)	751.8 [±71.4]*	90.6 [17.2%]
	JC1667	*ΔmutL Pxyl::YFP-mutL(D472N)* (endonuclease)	904.3 [±204.2]*	109.0 [0.4%]
D	JC1870	*ΔuvrD Pxyl::YFP-uvrD*	102.5 [±39.5]#	12.3 [82.3%]

Supplementary Figures:

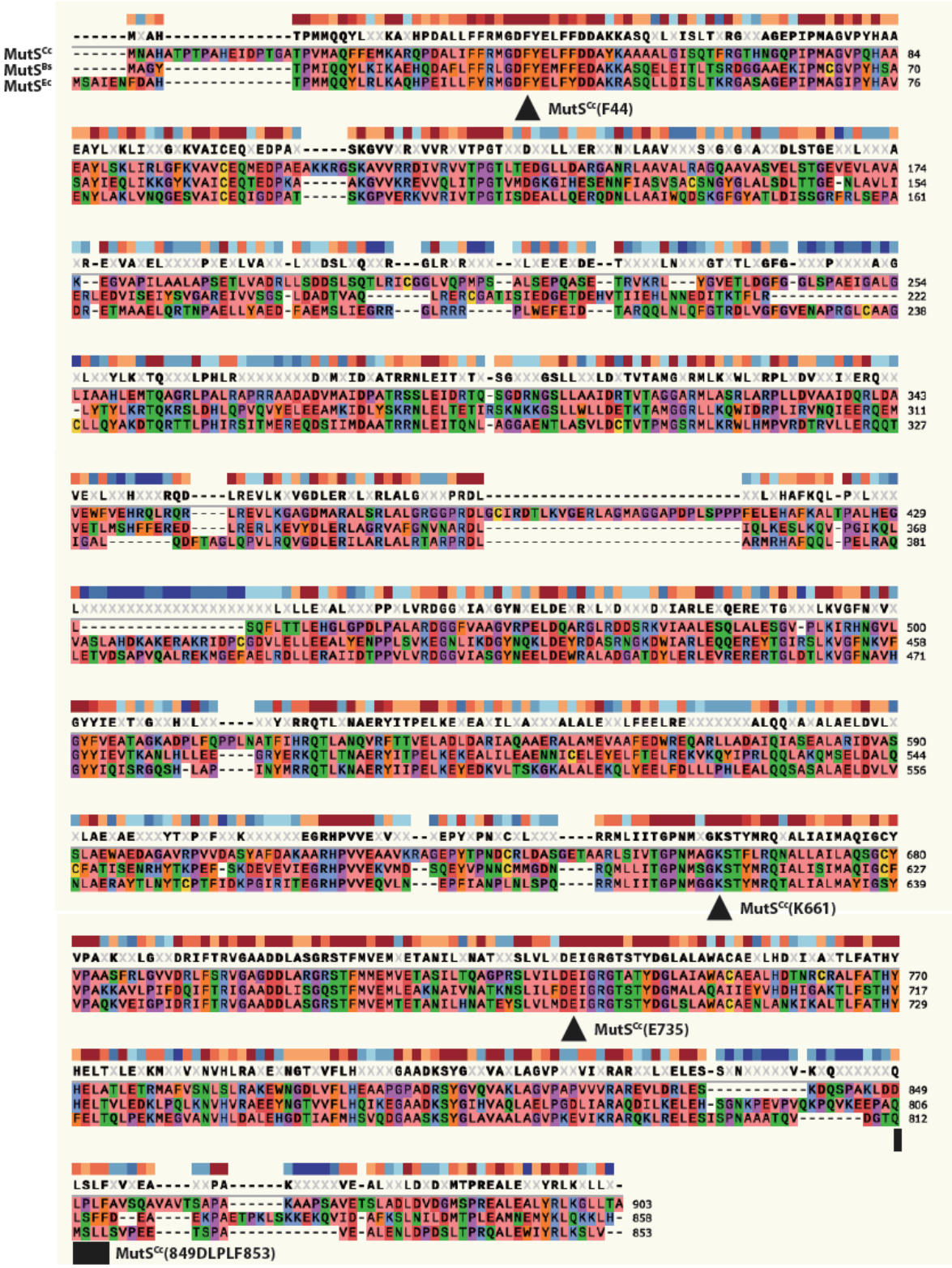

Figure S1: Similarities between selected MutS proteins. Amino-acid sequences of MutS homologs were downloaded from NCBI for *Caulobacter crescentus* NA1000 strain (MutS^{Cc}), *Bacillus subtilis* PY79 strain (MutS^{Bs}) and *Escherichia coli* MG1655 strain (MutS^{Ec}).

Alignments were done using the SnapGene software (from Insightful Science; available at snapgene.com). $MutS^{Cc}$ residues/motifs of particular interest are indicated under the three sequences. The F44 residue belongs to a $_{42}$GDFYELFFDDA$_{52}$ motif where underlined residues are part of the consensus motif for mismatch recognition by MutS proteins (4). The K661 residue belongs to a $_{655}$GPNMAGKS$_{662}$ Walker A motif supposedly involved in ATP/ADP binding and whose consensus is GxxxxGK[T/S] (x can be any amino acid) (5). The E735 residue belongs to a $_{689}$LVLMDE$_{694}$ Walker B motif supposedly involved in ATP hydrolysis and whose consensus is hhhhDE (h is a hydrophobic amino acid) (5). The $_{849}$DLPFL$_{853}$ motif shows similarities with the β-clamp binding motifs $MutS^{Bs}$ ($_{806}$QLSFF$_{810}$) (6)and $MutS^{Ec}$ ($_{812}$QMSLL$_{816}$) (7).

Figure S2: Similarities between selected MutL proteins. Amino-acid sequences of MutL homologs were downloaded from NCBI for *Caulobacter crescentus* NA1000 strain (MutS^{Cc}), *Bacillus subtilis* PY79 strain (MutS^{Bs}) and *Escherichia coli* MG1655 strain (MutS^{Ec}). Alignments were done using the SnapGene software. MutL^{Cc} residues/motifs of particular interest are indicated under the three sequences. The D472 residue belongs to the predicted $_{472}$DQHAAHERLVYE$_{483}$ endonuclease domain (underlined letters indicate conserved residues according to (8)). The $_{497}$QTLLLP$_{502}$ motif shows similarities with the previously proposed Qxh(L/I)xP consensus β-clamp binding motif for MutL proteins (9).

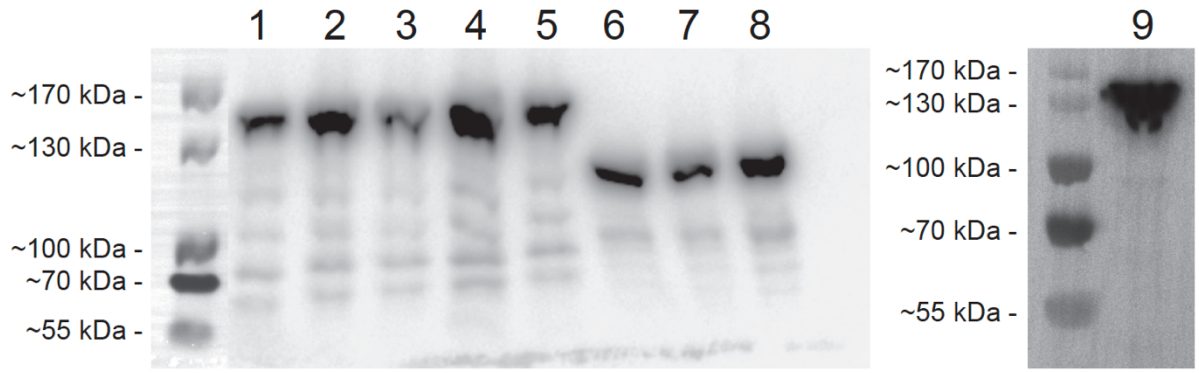

Figure S3: Immunoblot detection of YFP-tagged MutS, MutL and UvrD derivatives from *C. crescentus* cell extracts. Cells from strains JC1433 (Δ*mutS Pxyl::YFP-mutS*) (Lane 1), JC1665 (Δ*mutS Pxyl::YFP-mutS(K661M)*) (Lane 2), JC1666 (Δ*mutS Pxyl::YFP-mutS(F44A)*) (Lane 3), JC1739 (Δ*mutS Pxyl::YFP-mutS(E735A)*) (Lane 4), JC1770 (Δ*mutS Pxyl::YFP-mutS*($_{849}$*AAAAA*$_{853}$)) (Lane 5), JC1825 (Δ*mutL Pxyl::YFP-mutL*) (Lane 6), JC1667 (Δ*mutL Pxyl::YFP-mutL(D472N)*) (Lane 7), JC1749 (Δ*mutL Pxyl::YFP-mutL*($_{497}$*ATLAAP*$_{502}$)) (Lane 8) and JC1870 (Δ*uvrD Pxyl::YFP-uvrD*) (Lane 9) were cultivated overnight in PYE medium before the culture was diluted into M2G medium. Once the OD_{660nm} reached ~0.3 (mid-exponential phase), 0.3% xylose was added. Cell extracts were then prepared when cultures reached an OD_{660nm} of ~0.5 (exponential phase) and proteins were separated by SDS-PAGE. YFP-tagged proteins were then detected by immunoblotting using anti-GFP antibodies. MW corresponds to the molecular weight in kDa. This figure shows that the YFP moiety of each fusion protein is not cleaved off.

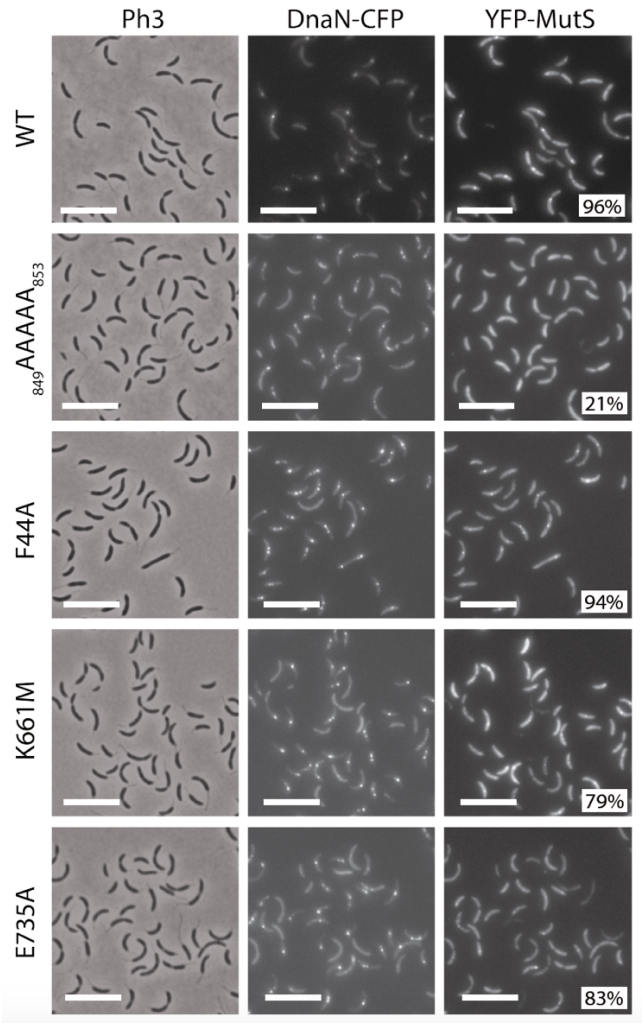

Figure S4: YFP-MutS foci co-localize with the replisome in *C. crescentus*. Subcellular localization of DnaN-CFP and derivatives of YFP-MutS in Δ*mutS* cells. Strains JC1625 (Δ*mutS dnaN-CFP Pxyl::YFP-mutS*), JC1771 (Δ*mutS dnaN-CFP Pxyl::YFP-mutS(*$_{849}$*AAAAA*$_{853}$*)*), JC1669 (Δ*mutS dnaN-CFP Pxyl::YFP-mutS(F44A)*), JC1668 (Δ*mutS dnaN-CFP Pxyl::YFP-mutS(K661M)*) and JC1740 (Δ*mutS dnaN-CFP Pxyl::YFP-mutS(E735A)*) were cultivated into PYE medium and then transferred into M2G medium. 0.3% xylose was added to cultures when they reached an OD_{660nm}~0.3. Cells were then imaged by fluorescence microscopy when the OD_{660nm} reached ~0.5. The % indicated onto images corresponds to the average proportion of distinct MutS-YFP foci (intensity >2-fold above background) that are co-localized with DnaN-CFP foci (using values obtained from three independent experiments). The white scale bar corresponds to 8µm.

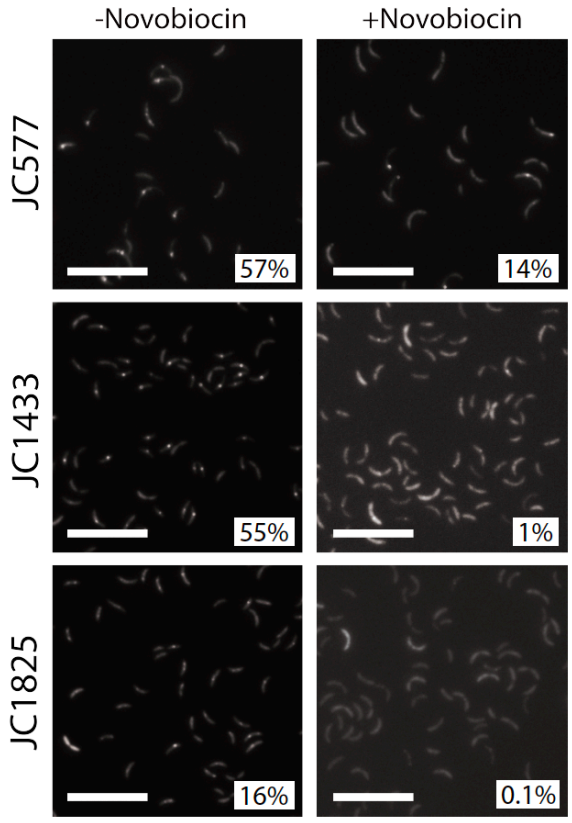

Figure S5: Replication inhibition following novobiocin treatment largely dissociates DnaN-CFP, YFP-MutS and YFP-MutL foci. Strains JC577 (*dnaN-CFP*), JC1433 (Δ*mutS Pxyl::YFP-mutS*) and JC1825 (Δ*mutL Pxyl::YFP-mutL*) were cultivated in PYE medium and then transferred into M2G medium. When the OD_{660nm} reached ~0.3, cultures were split into two and 100 µg/mL of novobiocin was added into one of the sub-cultures. 0.3% xylose was added at the same time into each sub-cultures of strains JC1433 and JC1825. Once the OD_{660nm} of the sub-culture without novobiocin reached 0.5, cells were imaged by fluorescence microscopy using CFP (for DnaN-CFP) or YFP (for YFP-MutS or YFP-MutL) illumination. Representative images are shown here. % indicated under each image correspond to the average proportion of cells displaying CFP or YFP foci (intensity >2-fold above background) as counted during three independent experiments. The white scale bar corresponds to 11µm.

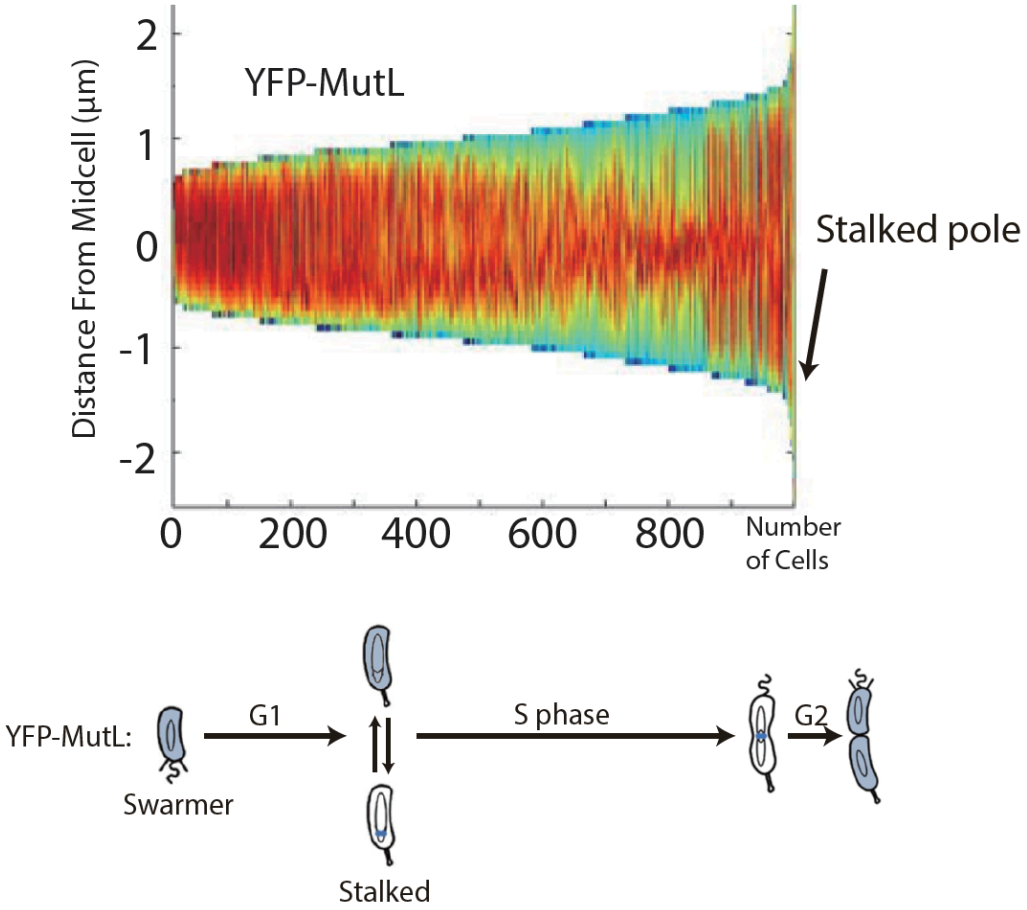

Figure S6: YFP-MutL is enriched at mid-cell towards the end of the S-phase of the *C. crescentus* cell cycle. Demograph showing the subcellular localization of YFP-MutL in Δ*mutL* cells sorted as a function of their size. JC1825 (Δ*mutL Pxyl::YFP-mutL*) cells were cultivated and imaged as described for Fig.5A. Short cells correspond to G1/swarmer cells, while intermediate and longer cells correspond to stalked and pre-divisional S-phase cells, respectively. The schematic under the demograph shows the *C. crescentus* cell cycle and the blue color highlights where YFP-MutL seems to be localized as a function of the cell cycle.

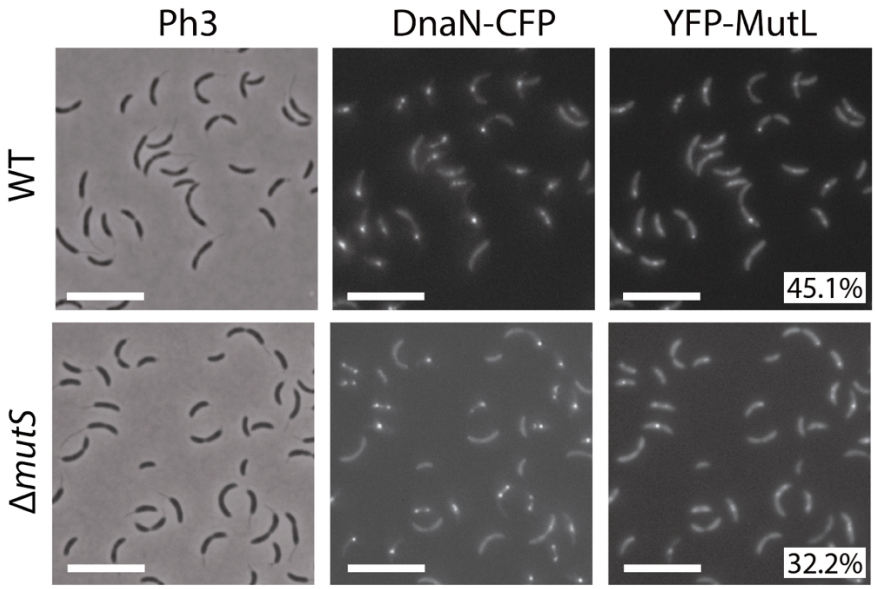

Figure S7: YFP-MutL is recruited to the replisome independently of MutS. Subcellular localization of DnaN-CFP and YFP-MutL in Δ*mutL* cells with or without *mutS*. Strains JC1812 (*dnaN-CFP* Δ*mutL Pxyl::YFP-mutL*) labelled "WT" and JC1805 (*ΔmutS* Δ*mutL dnaN-CFP Pxyl::YFP-mutL*) labelled *"ΔmutS*" were cultivated into PYE medium and then transferred into M2G medium. 0.3% xylose was added to cultures when they reached an OD_{660nm}~0.3. Cells were then imaged by fluorescence microscopy when the OD_{660nm} reached ~0.5. The % indicated onto images corresponds to the average proportion of cells with distinct MutL-YFP foci (intensity >2-fold above average background) using values obtained from three independent experiments. The white scale bar corresponds to 8µm.

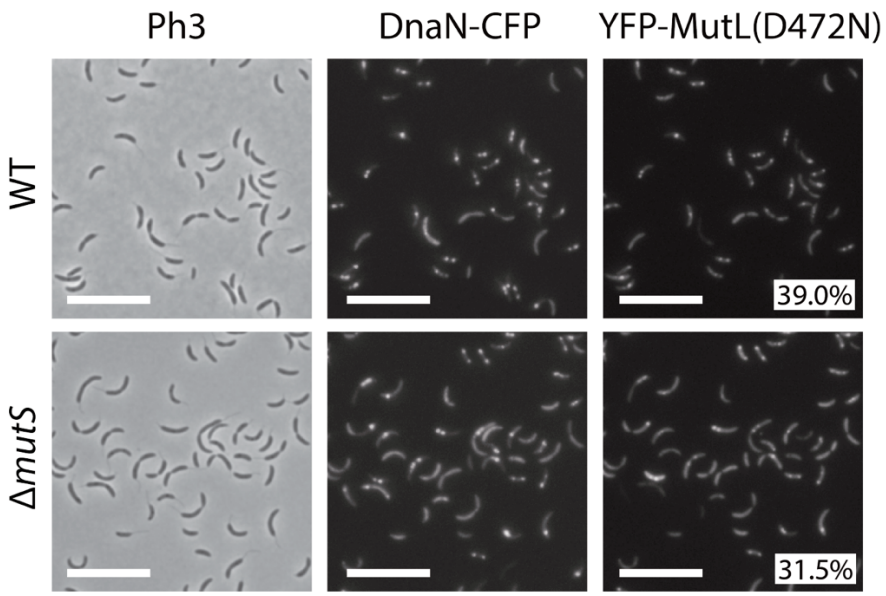

Figure S8: YFP-MutL(D472N) is stabilized at the replisome even in the absence of MutS. Subcellular localization of DnaN-CFP and YFP-MutL(D472N) in Δ*mutL* cells with or without *mutS*. Strains JC1670 (Δ*mutL dnaN-CFP Pxyl::YFP-mutL (D472N)*) and JC1894 (*ΔmutS ΔmutL dnaN-CFP Pxyl::YFP-mutL (D472N)*) were cultivated into PYE medium and then transferred into M2G medium. 0.3% xylose was added to cultures when they reached an OD_{660nm}~0.3. Cells were then imaged by fluorescence microscopy when the OD_{660nm} reached ~0.5. The % indicated onto images corresponds to the average proportion of cells with distinct MutL-YFP(D472N) foci (intensity >2-fold above average background) using values obtained from three independent experiments. The white scale bar corresponds to 11µm.

Supplementary Material and Methods

Plasmids constructions

Derivatives of pNPTS138:

To construct pNPTS138-ΔmutS, pNPTS138-ΔmutL and pNPTS138-ΔuvrD, ~500 bp sequences upstream and downstream of the corresponding ORF were amplified by PCR from wild-type *C. crescentus* chromosomal DNA using the primer pairs listed in Table S1. The two fragments were subsequently digested by restriction enzymes (as indicated in Table S1) and cloned into the pNPTS138 suicide vector between corresponding restriction sites by triple ligation.

To construct pNPTS138-DnaQ(G13E), pNPTS138-MutS($_{849}$AAAAA$_{853}$) and pNPTS138-MutL($_{497}$ATLAAP$_{503}$), overlap extension PCR were used to construct ~1 kb gene fragment with the required mutations in *dnaQ*, *mutS* or *mutL*. The PCR consisted of two consecutive PCR reactions, with four primers (listed in Table S1).

To construct pNPTS138-PmutS-YFP-mutS and pNPTS138-PmutL-YFP-mutL, two primer pairs (listed in Table S1) were used to amplify the ~500 bp promoter regions (PmutS and PmutL, respectively) and the protein fusion regions (YFP-mutS and YFP-mutL, respectively). The two fragments were subsequently digested by the indicated restriction enzymes (Table S1) and cloned into the pNPTS138 suicide vector between corresponding restriction sites by triple ligation.

Derivatives of pXYFPN4:

To construct pXYFPN4-MutS, pXYFPN4-MutL and pXYFPN4-UvrD, the corresponding ORFs were amplified by PCR from wild-type *C. crescentus* chromosomal DNA using the primer pairs listed in Table S1, digested by the indicated restriction enzymes and cloned into pXYFPN4.

To construct pXYFPN4-MutS(F44A), pXYFPN4-MutS(K661M), pXYFPN4-MutS(E735A), pXYFPN4-MutS($_{849}$AAAAA$_{853}$), pXYFPN4-MutL(D472N), pXYFPN4-MutL($_{497}$ATLAAP$_{502}$) and pXYFPN4-MutL(D472N , $_{497}$ATLAAP$_{502}$) overlap PCR was used to construct a point mutation in the *mutS* or *mutL* genes. Two consecutive PCR reactions were performed using four primers (listed in Table S1). First, two DNA fragments were amplified from plasmid pXYFPN4-mutS (for *mutS* alleles) or pXYFPN4-mutL (for *mutL* alleles). Then, equimolar amounts of both products were mixed and amplified. The resulting fragments were digested by restriction enzymes (as indicated in Table S1) and cloned into the pXYFPN4 vector.

Strains constructions

Three categories of strains were constructed: (1) gene deletions or gene replacements were constructed using pNPTS138-derived plasmids (listed in Table S2) via two homologous recombination events: first, the suicide vectors were integrated at the desired location into the genome via homologous recombination and selection for kanamycin resistance. Excision of the suicide vector via a second homologous recombination event was then selected by plating on sucrose (0.3%)-containing PYEA plates and the isolated colonies were subsequently selected for kanamycin sensitivity. The mutants were identified by PCR using primer pairs used to construct pNPTS138 derivatives (Table S1) or by DNA sequencing for gene replacements; (2) pXYFPN4 derivatives were integrated at the native *xylX* locus by transformation. Positive clones were screened using RecUni-1 and RecXyl-2 primers (1). These strains were used for the inducible expression of MutS, MutL, UvrD derivatives in the presence of 0.3% xylose; (3) In JC1724, JC1845 and JC2211, the pNPTS138-DnaQ-G13E plasmid was integrated at the native *dnaQ* locus. The resulting strains express the *dnaQ(G13E)* allele together with a truncated and inactive *dnaQ*' allele. Oligos TC34 and M13-F were used to check the integration sites of the plasmid.

Immunoblot analysis

YFP-tagged proteins were resolved on 8% SDS-PAGE gels. Proteins were then transferred to PVDF membranes (Millipore). Two antibodies were used for immunodetection: Anti-GFP antibody (GFP Tag Antibody, GF28R, Mouse IgG, Thermo Fisher) was diluted 1:3000 and Anti-Mouse IgG HRP Conjugate (Promega) was diluted 1:5000. The signal was visualized using a chemiluminescent reagent (Amersham ECL Prime Western Blotting Detection Reagent, GE) and a FUSION FX (VILBER) scanner. Images were processed by Photoshop.

Supplementary References

1. Thanbichler, M., Iniesta, A.A. and Shapiro, L. (2007) A comprehensive set of plasmids for vanillate- and xylose-inducible gene expression in *Caulobacter crescentus*. *Nucleic Acids Res*, **35**, e137.
2. Evinger, M. and Agabian, N. (1977) Envelope-associated nucleoid from *Caulobacter crescentus* stalked and swarmer cells. *J Bacteriol*, **132**, 294-301.

3. Fernandez-Fernandez, C., Grosse, K., Sourjik, V. and Collier, J. (2013) The beta-sliding clamp directs the localization of HdaA to the replisome in *Caulobacter crescentus*. *Microbiology*, **159**, 2237-2248.
4. Lenhart, J.S., Sharma, A., Hingorani, M.M. and Simmons, L.A. (2013) DnaN clamp zones provide a platform for spatiotemporal coupling of mismatch detection to DNA replication. *Mol Microbiol*, **87**, 553-568.
5. Hanson, P.I. and Whiteheart, S.W. (2005) AAA+ proteins: have engine, will work. *Nat Rev Mol Cell Biol*, **6**, 519-529.
6. Simmons, L.A., Davies, B.W., Grossman, A.D. and Walker, G.C. (2008) Beta clamp directs localization of mismatch repair in *Bacillus subtilis*. *Mol Cell*, **29**, 291-301.
7. Lopez de Saro, F.J., Marinus, M.G., Modrich, P. and O'Donnell, M. (2006) The beta sliding clamp binds to multiple sites within MutL and MutS. *J Biol Chem*, **281**, 14340-14349.
8. Pillon, M.C., Lorenowicz, J.J., Uckelmann, M., Klocko, A.D., Mitchell, R.R., Chung, Y.S., Modrich, P., Walker, G.C., Simmons, L.A., Friedhoff, P. *et al.* (2010) Structure of the Endonuclease Domain of MutL: Unlicensed to Cut. *Mol Cell*, **39**, 145-151.
9. Pillon, M.C., Miller, J.H. and Guarne, A. (2011) The endonuclease domain of MutL interacts with the beta sliding clamp. *DNA Repair*, **10**, 87-93.